LAL 02-103
December 21, 2002

Interpreting CP Asymmetries in $B^0 \to \pi^+\pi^-$ Decays

Andreas Höcker[(a)], Heiko Lacker[(a)], Muriel Pivk[(b)], Lydia Roos[(b)]

[(a)] *Laboratoire de l'Accélérateur Linéaire, IN2P3-CNRS et Université de Paris-Sud, BP 34, F-91898 Orsay Cedex, France*

[(b)] *LPNHE-Paris, IN2P3-CNRS et Université de Paris VI-VII, Tour 33 rdc, 4 place Jussieu, 75232 Paris cedex 05, France*

Abstract

We discuss methods to interpret the measurements of CP-asymmetry in $B^0 \to \pi^+\pi^-$ within the Standard Model. Various theoretical frameworks are considered, starting from the rather general, yet unpredictive properties based on strong isospin symmetry, reaching to highly predictive calculations using QCD Factorization. For each case study, the corresponding constraints on the phase of the CKM matrix, experimental observables and phenomenological parameters are presented. The calculations are performed using the software package *CKMfitter* featuring the frequentist statistical approach *R*fit.

1 Introduction

Unlike the measurement of $\sin 2\beta$ from $B^0 \to J/\psi K_S^0$ or similar decays, for which processes with weak phases that are different from the dominant tree phase are doubly Cabibbo suppressed, multiple weak phases have to be considered in the analyses of charmless B decays aiming at the extraction of $\sin 2\alpha$. This note discusses the physical implications of the *BABAR* and Belle results on time-dependent *CP*-violating asymmetries in $B^0 \to \pi^+\pi^-$, taking into account averaged results on branching fractions and direct *CP* asymmetries of $B \to hh'$ decays (h, h' denoting neutral or charged pions or kaons). We attempt herein:

- to provide a clear-cut definition of the contributing amplitudes and their weak and strong phases,
- to recall the most important relations among them (unitarity, isospin, SU(3), etc.),
- to interpret the results with an increasing input of experimental and theoretical constraints.

The computational work has been carried out using the program package *CKMfitter* [1]. It features the statistical approach *R*fit, which is based on a frequentist understanding of systematic theoretical uncertainties. Theoretical parameters are treated as freely varying, bound or unbound dependents in the fit.

In general, the constraints are presented in the parameter spaces $(\bar\rho, \bar\eta)$, the unitarity triangle angle α, the plane spanned by the observed coefficients of the sine and the cosine terms, $(S_{\pi\pi}, C_{\pi\pi})$, as well as the relative strong phase vs. the penguin-to-tree ratio, $(|P/T|, \delta_{\pi\pi})$. It is the goal of the latter two representations to test theoretical approaches used to describe the dynamical structure of the transition amplitudes. A priori knowledge on the CKM phase, obtained from the standard CKM analysis [1] (see Appendix B for a brief review of the relevant SM fit inputs), is injected into these fits, either for comparison purposes, or as direct input to predict experimentally accessible observables or theoretical quantities.

We approach the problem following the hierarchical structure outlined below:

(I) using as input $S_{\pi\pi}$ and $C_{\pi\pi}$ as well the branching fractions $B \to \pi\pi$ (all charges) and strong isospin symmetry SU(2) and neglecting electro-weak penguins.

(II) using (I) and $B^0 \to K^+\pi^-$ together with $SU(3)$ flavour symmetry and neglecting OZI-suppressed penguin annihilation topologies.

(III) using (I) and a phenomenological estimate of $|P|$ by means of the decay rate $B^+ \to K^0\pi^+$, assuming "naive factorization" to estimate SU(3) breaking; the relative strong phase is unconstrained in this approach.

(IV) using (I) and the prediction of the complex penguin-to-tree ratio, that is $|P/T|$ and its phase, predicted by QCD Factorization.

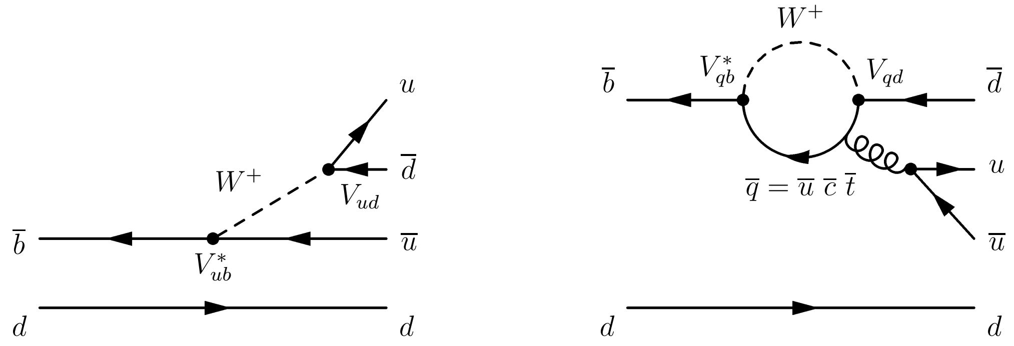

Figure 1: *Tree (left) and penguin (right) diagrams for the decay* $B^0 \to \pi^+\pi^-$.

Throughout this note, we will assume that *CP* violation in mixing is absent, *i.e.*, $|q/p| = 1$, as suggested by the Standard Model ($|\Gamma_{B_H} - \Gamma_{B_L}| \ll \Gamma_{B^0}$), and found by *BABAR* to be $|q/p| = 0.998 \pm 0.006 \pm 0.007$ [2].

2 Basic Formulae and Definitions

We use in general the conventions adopted in Refs. [3, 4, 5]. However, since the results are to be translated into constraints on the CKM phase, care has to be taken to properly factorize the CKM elements occurring at the weak vertices. The complex Standard Model amplitudes of the relevant processes represent the sum of tree (T) and penguin (P) amplitudes with different weak and strong phases, in general. The corresponding Feynman diagrams for the decay $B^0 \to \pi^+\pi^-$ are depicted in Fig. 1. Exchange diagrams (see Fig. 5) are included in the tree since they have the same weak phase. The transition amplitudes are given by[1]

$$A^{+-} \equiv A(B^0 \to \pi^+\pi^-) = R_u e^{i\gamma} T^{+-} + R_t e^{-i\beta} P^{+-} , \quad (1)$$

$$\overline{A}^{+-} \equiv A(\overline{B}^0 \to \pi^+\pi^-) = R_u e^{-i\gamma} T^{+-} + R_t e^{i\beta} P^{+-} , \quad (2)$$

where $T^{+-} = |T^{+-}|e^{i\delta_{T^{+-}}}$ and $P^{+-} = |P^{+-}|e^{i\delta_{P^{+-}}}$. The *CP* transformation alters the sign of the weak phase only, since the strong interaction is assumed to be *CP* conserving. The parameters R_u, R_t and, correspondingly R_c, measure the sides of the unitarity triangle (UT) sketched in Fig. 2. Adopting the Wolfenstein parameterization [6] one has[2]

$$R_u \equiv |V_{ud}V_{ub}^*| \simeq A\lambda^3\sqrt{\bar\rho^2 + \bar\eta^2} , \quad (3)$$

$$R_c \equiv |V_{cd}V_{cb}^*| \simeq A\lambda^3 , \quad (4)$$

[1] We have used unitarity to reorganize the c, u and t penguin amplitudes according to their weak phases in the tree and penguin components of Eqs. (1,2). See Section 2.1 for a detailed discussion.

[2] The length of the vector to the triangle apex is given by $\left|\frac{V_{ud}V_{ub}^*}{V_{cd}V_{cb}^*}\right| = \sqrt{\rho^2+\eta^2}\left(1-\frac{\lambda^2}{2}\right) + O(|\lambda|^4)$, so that the replacements $\rho \to \rho(1-\lambda^2/2)$ and $\eta \to \eta(1-\lambda^2/2)$, where $V_{ud} = 1-\lambda^2/2 - O(\lambda^4)$, improves the precision of the apex coordinate in the Wolfenstein approximation [7].

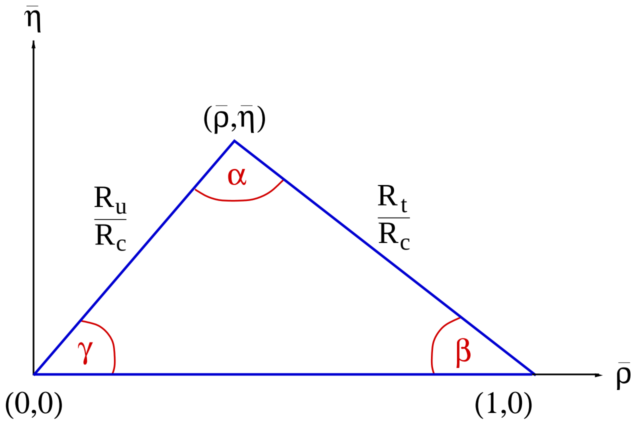

Figure 2: *The rescaled Unitarity Triangle in the Wolfenstein parameterization.*

$$R_t \equiv |V_{td}V_{tb}^*| \quad \simeq \quad A\lambda^3\sqrt{(1-\bar{\rho})^2+\bar{\eta}^2} \ , \tag{5}$$

where $V_{td} = |V_{td}|e^{-i\beta}$ and $V_{ub} = |V_{ub}|e^{-i\gamma}$, with β and γ being the bottom angles of the UT, *i.e.*, $\tan\beta = \bar{\eta}/(1-\bar{\rho})$ and $\tan\gamma = \bar{\eta}/\bar{\rho}$ (note also that $\delta = \gamma$, where δ is the CKM phase in the standard parameterization adopted by the PDG). The time-dependent *CP* asymmetry of the physical $B^0\overline{B}^0$ system is given by

$$\begin{aligned} a_{CP}(\Delta t) \quad &\equiv \quad \frac{\Gamma(\overline{B}^0_{\rm phys}(\Delta t)\to\pi^+\pi^-) - \Gamma(B^0_{\rm phys}(\Delta t)\to\pi^+\pi^-)}{\Gamma(\overline{B}^0_{\rm phys}(\Delta t)\to\pi^+\pi^-) + \Gamma(B^0_{\rm phys}(\Delta t)\to\pi^+\pi^-)} \\ &= \quad S_{\pi\pi}\sin(\Delta m_d\Delta t) - C_{\pi\pi}\cos(\Delta m_d\Delta t) \ , \end{aligned} \tag{6}$$

where Δm_d is the $B^0\overline{B}^0$ oscillation frequency, Δt is the time difference between the *CP* and the tag side decays, and the coefficients of the sine and cosine terms are given by

$$S_{\pi\pi} = \frac{2{\rm Im}\lambda_{\pi\pi}}{1+|\lambda_{\pi\pi}|^2} \quad \text{and} \quad C_{\pi\pi} = \frac{1-|\lambda_{\pi\pi}|^2}{1+|\lambda_{\pi\pi}|^2} \ . \tag{7}$$

The *CP* parameter $\lambda_{\pi\pi}$ is given by the standard expression (we recall that it is assumed $|q/p| = 1$)

$$\lambda_{\pi\pi} = e^{-2i\beta}\frac{\overline{A}^{+-}}{A^{+-}} \ , \tag{8}$$

where the phase $e^{-2i\beta}$ arises due to $B^0\overline{B}^0$ mixing. Eq. (8) implies that $\pi^+\pi^-$ is a *CP* eigenstate with eigenvalue $+1$.

In absence of penguin contributions ($P = 0$), Eq. (8) reduces to $\lambda_{\pi\pi} = e^{2i\alpha}$ (using the triangle relation $\alpha+\beta+\gamma=\pi$) and hence:

$$S_{\pi\pi}[P=0] = \sin 2\alpha \quad \text{and} \quad C_{\pi\pi}[P=0] = 0 \ . \tag{9}$$

In the presence of penguin contributions, the phase of $\lambda_{\pi\pi}$ is modified by the relative strong phase $\delta_{\pi\pi} \equiv \arg(P^{+-}T^{+-*})$ between the penguin and the tree amplitudes. In addition, the parameter $C_{\pi\pi}$ will be non-zero (if $\delta_{\pi\pi} \neq 0$), thus measuring the occurrence of direct *CP* violation[3]. Defining an effective angle $\alpha_{\rm eff}$ that incorporates the phase shift ($r^{+-} \equiv (R_t/R_u)|P^{+-}/T^{+-}|$):

$$\lambda_{\pi\pi} = e^{2i\alpha}\frac{1 - r^{+-}\,e^{-i(\alpha-\delta_{\pi\pi})}}{1 - r^{+-}\,e^{+i(\alpha+\delta_{\pi\pi})}} \equiv |\lambda_{\pi\pi}|e^{2i\alpha_{\rm eff}} \ , \tag{10}$$

one finds, using $|\lambda_{\pi\pi}| = \sqrt{1-C_{\pi\pi}}/\sqrt{1+C_{\pi\pi}}$ (see Eq. 7),

$$S_{\pi\pi} = \sqrt{1-C_{\pi\pi}^2}\sin 2\alpha_{\rm eff} \ . \tag{11}$$

Twice of the effective angle $\alpha_{\rm eff}$ corresponds to the relative phase between the amplitudes $e^{-2i\beta}\overline{A}^{+-}$ and A^{+-} . It is useful for the following to define the phase difference

$$\theta \equiv \alpha - \alpha_{\rm eff} \ . \tag{12}$$

2.1 Unitarity relations

In general, the penguin amplitude accounts for the three up-type quark flavours, u, c, t, occurring in the W loop (see right hand plot in Fig. 1), so that the general form of Eq. (1) reads

$$A^{+-} \equiv A(B^0 \to \pi^+\pi^-) = R_u e^{i\gamma}T_u + R_u e^{i\gamma}P_u + R_c e^{i\pi}P_c + R_t e^{-i\beta}P_t \ . \tag{13}$$

In the definitions (1-2) (we have used the fact that in the standard CKM phase convention the u penguin has the same weak phase γ as the tree amplitude). Moreover, we have benefited from the unitarity relation between the first and the third column of the CKM matrix,

$$V_{ud}V_{ub}^* + V_{cd}V_{cb}^* + V_{td}V_{tb}^* = 0 \ , \tag{14}$$

to eliminate the c penguin[4]. The particular choice which penguin to remove in the definition of a transition amplitude is arbitrary and does not have observable physical implications. However, the convention does modify the contents of the phenomenological amplitudes T^{+-} and P^{+-} introduced in (1).

In terms of the Wolfenstein parameterization to the order $O(\lambda^5)$, Eq. (14) reads[5]

$$R_u e^{i\gamma} + R_c e^{i\pi} + R_t e^{-i\beta} = A\lambda^3(\bar\rho + i\bar\eta) - A\lambda^3 + A\lambda^3(1-\bar\rho-i\bar\eta) = 0 \ . \tag{15}$$

[3] It is *direct CP* violation, since $|\overline{A}^{+-}/A^{+-}| \neq 1$, if $C_{\pi\pi} \neq 0$.

[4] Note that penguin amplitudes are intrinsically divergent and only differences in penguin operators lead to finite results (see, *e.g.*, Ref. [3]).

[5] The sides of the UT (15) are of the same order in λ, thus predicting large *CP*-violating phases in the B system. As a comparison, the corresponding UT for the kaon sector is almost flat,

$$V_{ud}V_{us}^* + V_{cd}V_{cs}^* + V_{td}V_{ts}^* \simeq \lambda - \lambda - A^2\lambda^5(1-\bar\rho-i\bar\eta) = 0 \ ,$$

exhibiting small relative *CP* asymmetries.

Inserting Eq. (15) into (13), we obtain the three solutions $\mathfrak{U}$, $\mathfrak{C}$, $\mathfrak{T}$:

$$A^{+-} = \begin{cases} R_u e^{i\gamma} T_u + R_c(P_u - P_c) + R_t e^{-i\beta}(P_t - P_u) & (\mathfrak{U}) \\ R_u e^{i\gamma}(T_u + P_u - P_c) + R_t e^{-i\beta}(P_t - P_c) & (\mathfrak{C}) \\ R_u e^{i\gamma}(T_u + P_u - P_t) + R_c(P_t - P_c) & (\mathfrak{T}) \end{cases} \tag{16}$$

for which the u ($\mathfrak{U}$), c ($\mathfrak{C}$) and t ($\mathfrak{T}$) penguin coefficients have been substituted respectively. In effect, Eq. (1) corresponds to eliminating the phaseless c piece (solution $\mathfrak{C}$) from the general ansatz (13), thus implying that

$$T^{+-} \equiv T_u + P_u - P_c \quad \text{and} \quad P^{+-} \equiv P_t - P_c \ . \tag{17}$$

Another convenient choice, frequently found in the literature is solution $\mathfrak{T}$, since only one unknown weak phase is left.

2.2 Direct CP violation

With the assumption of $|q/p| = 1$, the direct *CP*-violating parameter $C_{\pi\pi}$ measures the asymmetry

$$C_{\pi\pi} = \frac{|A^{+-}|^2 - |\overline{A}^{+-}|^2}{|A^{+-}|^2 + |\overline{A}^{+-}|^2} \ . \tag{18}$$

Inserting the amplitude convention $\mathfrak{C}$ (*cf.* Eq. (16)), one has

$$C_{\pi\pi} = \frac{2R_uR_t|T^{(\mathfrak{C})}||P^{(\mathfrak{C})}|\sin(\beta+\gamma)\sin\delta^{(\mathfrak{C})}}{R_u^2|T^{(\mathfrak{C})}|^2 + R_t^2|P^{(\mathfrak{C})}|^2 + 2R_uR_t|T^{(\mathfrak{C})}||P^{(\mathfrak{C})}|\cos(\beta+\gamma)\cos\delta^{(\mathfrak{C})}} \ , \tag{19}$$

and for convention $\mathfrak{T}$ one finds

$$C_{\pi\pi} = \frac{2R_uR_c|T^{(\mathfrak{T})}||P^{(\mathfrak{T})}|\sin\gamma\sin\delta^{(\mathfrak{T})}}{R_u^2|T^{(\mathfrak{T})}|^2 + R_c^2|P^{(\mathfrak{T})}|^2 + 2R_uR_c|T^{(\mathfrak{T})}||P^{(\mathfrak{T})}|\cos\gamma\cos\delta^{(\mathfrak{T})}} \ , \tag{20}$$

where $T^{(\mathfrak{C})} = T^{+-}$, $P^{(\mathfrak{C})} = P^{+-}$, $T^{(\mathfrak{T})} = T^{+-} + P_c - P_t = T^{+-} - P^{+-}$, $P^{(\mathfrak{T})} = P^{+-}$, and T^{+-}, P^{+-} are defined in Eq. (17). Of course, as a consequence of unitarity, Eqs. (19) and (20) must be equal. This can be verified by means of the relations (*cf.* Eq. (15))

$$\sin(\beta+\gamma) = \frac{R_c}{R_t}\sin\gamma \ , \tag{21}$$

$$\cos(\beta+\gamma) = \frac{R_c}{R_t}\left(\cos\gamma - \frac{R_u}{R_c}\right) \ , \tag{22}$$

$$|T^{(\mathfrak{C})}|\sin\delta^{(\mathfrak{C})} = |T^{(\mathfrak{T})}|\sin\delta^{(\mathfrak{T})} \ . \tag{23}$$

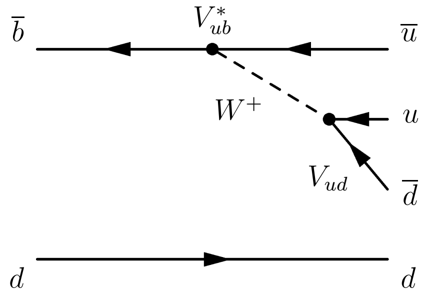

Figure 3: *Tree color-suppressed diagram for the decay $B^0 \to \pi^0\pi^0$.*

2.3 Isospin relations

Using strong isospin invariance, the amplitudes of the various $B \to \pi\pi$ decays are related to each other. Moreover, Gronau and London have shown [8] that the measurements of rates and CP asymmetries of the charged and two neutral $\pi\pi$ final states together with the exploitation of their isospin relations provides sufficient information to extract a up to an eightfold ambiguity (within $[0, 2\pi]$).

According to Eqs. (1-2) we can write

$$A^{+0} \equiv A(B^+ \to \pi^+\pi^0) = R_u e^{i\gamma}(T^{+0} + T_C^{+0}) + R_t e^{-i\beta} P_{\rm EW}^{+0} \,, \tag{24}$$

$$A^{00} \equiv A(B^0 \to \pi^0\pi^0) = R_u e^{i\gamma} T_C^{00} + R_t e^{-i\beta} P^{00} \,, \tag{25}$$

and changing the sign of the weak phases for the CP-conjugated modes. The C subscript stands for color suppressed amplitudes (see Fig. 3 for the color-suppressed tree diagram of the decay $B^0 \to \pi^0\pi^0$) and the EW subscript for the electroweak penguin amplitude contributing to $\pi^+\pi^0$. Note that electroweak penguins also contribute to the other $\pi\pi$ charges, but since they are in weak phase with the strong penguins we do not specify them in Eqs. (16) and elsewhere. Gluonic quark anti-quark production has $\Delta I = 0$ so that QCD penguins can only mediate $\Delta I = 1/2$ transitions of the b quark (see Appendix A). As a consequence, the $\Delta I = 3/2$ amplitude of the decay $B^+ \to \pi^+\pi^0$ has no strong penguin contribution. The occurrence of direct CP violation in this channel would thus imply significant electroweak (EW) penguins. Applying the isospin relations (*cf.* Appendix A)

$$A^{+0} = \frac{1}{\sqrt{2}} A^{+-} + A^{00} \,, \tag{26}$$

(and $A \leftrightarrow \overline{A}$, with $\overline{A}^{+0} = A^{-0}$) one can rearrange the amplitudes (24-25)

$$A^{+0} = R_u e^{i\gamma} \left(\frac{1}{\sqrt{2}} T^{+-} + T_C^{00} \right) + R_t e^{-i\beta} P_{\rm EW}^{+0} \,, \tag{27}$$

$$A^{00} = R_u e^{i\gamma} T_C^{00} - R_t e^{-i\beta} \left(\frac{1}{\sqrt{2}} P^{+-} - P_{\rm EW}^{+0} \right) \,. \tag{28}$$

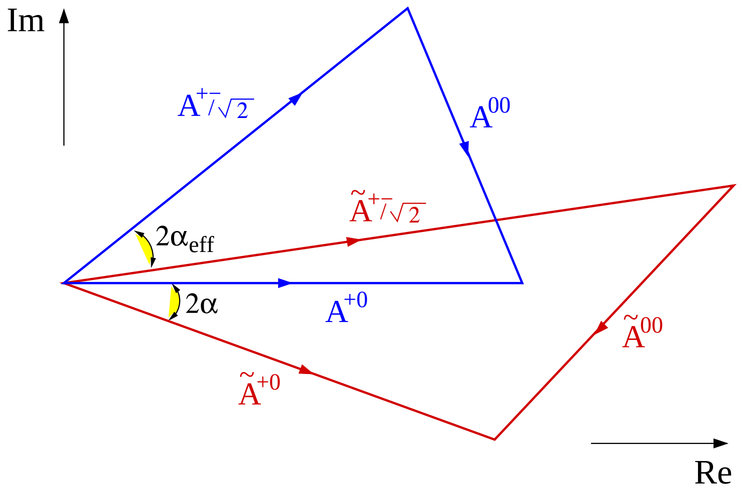

Figure 4: *The isospin relations (26) in the complex plane neglecting electroweak penguins (29). Note that a relative phase* $\arg(q/p) = -2\beta$ *due to* $B^0\overline{B}^0$ *mixing is added to the* $\overline{B}$ *triangle* ($\tilde{A}^{ij} \equiv e^{-2\beta}\overline{A}^{ij}$) .

Throughout this note, if not stated otherwise, all methods based on SU(2) symmetry assume that electroweak penguins can be neglected. In this case, one obtains

$$|A^{+0}| = |A^{-0}| \ . \tag{29}$$

The isospin relations between the three $\pi\pi$ amplitudes in the complex plane are depicted in Fig. 4. They represent two distinct triangles for the two *CP*-conjugated amplitudes whose A^{+0} and A^{+-} axes are rotated by 2γ and $2(\theta+\gamma)$, respectively. Taking into account the phase shift due to $B^0\overline{B}^0$ mixing, the relative rotation angles add up to 2α and $2\alpha_{\rm eff}$, respectively (as shown in the figure).

2.4 Bounds using SU(2) symmetry

Using the relations and definitions of Sec. 2.3 and the *CP*-averaged branching fractions

$$\mathcal{B}^{+-} = \frac{1}{2}\left(|A^{+-}|^2 + |\overline{A}^{+-}|^2\right) \ , \tag{30}$$

$$\mathcal{B}^{\pm 0} = \frac{1}{2}\left(|A^{+0}|^2 + |A^{-0}|^2\right) \ , \tag{31}$$

$$\mathcal{B}^{00} = \frac{1}{2}\left(|A^{00}|^2 + |\overline{A}^{00}|^2\right) \ , \tag{32}$$

(where the relation (29) implies $\mathcal{B}^{+0} = \mathcal{B}^{+0}$) one can deduce bounds on the relative strong phase $\delta_{\pi\pi}$ and $\mathcal{B}^{00}$. This has been first shown by Grossman-Quinn [9] and Charles [5]. It has been pointed out by Gronau-London-Sinha-Sinha [10] that the original bounds can be improved using the full information provided by the isospin relations (26) (in particular the closure of the isospin triangles) so that one obtains

$$\cos 2\theta \;\geq\; \frac{1-2\mathcal{B}^{00}/\mathcal{B}^{+0}}{y}+\frac{(\mathcal{B}^{+-}-2\mathcal{B}^{+0}+2\mathcal{B}^{00})^2}{4\mathcal{B}^{+-}\mathcal{B}^{+0}y}\;, \tag{33}$$

$$\cos 2\theta \;\geq\; \frac{1-4\mathcal{B}^{00}/\mathcal{B}^{+-}}{y}-\frac{(\mathcal{B}^{+-}-2\mathcal{B}^{+0}-2\mathcal{B}^{00})^2}{4\mathcal{B}^{+-}\mathcal{B}^{+0}y}\;, \tag{34}$$

where $y\equiv\sqrt{1-C_{\pi\pi}^2}$. The first terms on the right hand side of Eqs. (33-34) correspond to the original Charles limits, while the generally weaker Grossman-Quinn limit is obtained when further setting $y=1$. Following the same line it is possible to derive lower and upper bounds on the branching fraction into two neutral pions [10]:

$$\frac{1}{2}+\frac{\mathcal{B}^{+0}}{\mathcal{B}^{+-}}-\sqrt{\frac{\mathcal{B}^{+0}}{\mathcal{B}^{+-}}(1+y)}\;\leq\;\frac{\mathcal{B}^{00}}{\mathcal{B}^{+-}}\;\leq\;\frac{1}{2}+\frac{\mathcal{B}^{+0}}{\mathcal{B}^{+-}}+\sqrt{\frac{\mathcal{B}^{+0}}{\mathcal{B}^{+-}}(1+y)}\;, \tag{35}$$

where the limits are weakest for $y=1$, that is vanishing direct *CP* violation.

Note: although the evaluation of the above bounds provides interesting insight into the structure of the isospin relations, it is by no means a necessary exercise. Indeed, since no additional input is used it merely represents a reformulation of Eqs. (26). Analysis tools like *CKMfitter* automatically exploit the information from the bounds once they dispose of the input observables and the isospin relations. Moreover, *CKMfitter* guarantees the optimal use of the totality of the constraints given.

2.5 Improved bounds using SU(3) flavour symmetry

We extend the use of flavour symmetries to SU(3), considering the amplitude of the decay $B^0\to K^+\pi^-$ in $\mathfrak{C}$ convention

$$A_{K\pi}^{+-}\;\equiv\;A(B^0\to K^+\pi^-)\;=\;|V_{us}V_{ub}^*|e^{i\gamma}T_{K\pi}^{+-}+V_{ts}V_{tb}^*P_{K\pi}^{+-}\;. \tag{36}$$

Under the assumption of SU(3) flavour symmetry and neglecting OZI-suppressed penguin annihilation diagrams (see right hand diagram in Fig. 5), which contribute to $B^0\to\pi^+\pi^-$ but not to $B^0\to K^+\pi^-$, the penguin amplitudes in $B^0\to\pi^+\pi^-$ and $B^0\to K^+\pi^-$ are equal:

$$|P^{+-}|=|P_{K\pi}^{+-}|\;, \tag{37}$$

which leads to the bound [5]:

$$\cos 2\theta \;\geq\; \frac{1-2\lambda^2\mathcal{B}_{K\pi}^{+-}/\mathcal{B}^{+-}}{y}\;, \tag{38}$$

where λ is the Wolfenstein parameter.

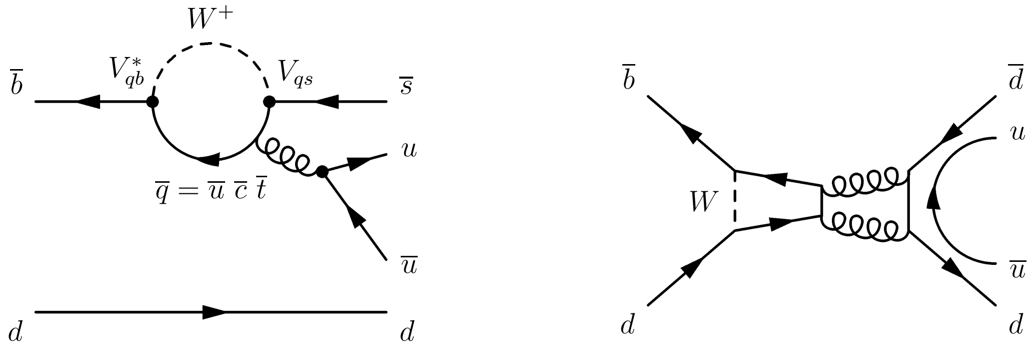

Figure 5: *Left: penguin diagram for the decay $B^0 \to K^+\pi^-$. Right: OZI-suppressed penguin annihilation diagram.*

Taking the world average for the corresponding branching fraction given in Table 2 yields $|\theta| \leq 29°$. Since the branching fractions for $B^0 \to \pi^+\pi^-$ and $B^0 \to K^+\pi^-$ are already measured with quite good precision the bound is not expected to improve significantly in the future. On the other hand, possibly large values for $C_{\pi\pi}$ might change the situation and lower the bound on θ.

Flavor symmetry SU(3) is only approximately realized in nature and one may expect violations of up to 30% on the amplitude level. For example, within factorization, the relative size of SU(3) symmetry breaking is expected to be $(f_K - f_\pi)/f_K$, with the pion and kaon decay constants $f_\pi = (130.7 \pm 0.4)$ MeV and $f_K = (159.8 \pm 1.4)$ MeV [12]. Notwithstanding, the bound in Eq. (38) can be considered conservative with respect to SU(3) breaking, since a correction would strengthen the bound. For example, under the assumption of factorization, the ratio of branching fractions $\mathcal{B}_{K\pi}^{+-}/\mathcal{B}^{+-}$ would be lowered by a factor $(f_\pi/f_K)^2 \simeq 0.67$.

2.6 Estimating $|P^{+-}|$ from $B^+ \to K^0\pi^+$

The ratio $|P^{+-}/T^{+-}|$ can be estimated using theoretical assumptions beyond those discussed in the previous section [5]. The penguin $|P^{+-}|$ is inferred from the branching fraction of the penguin-only mode $B^+ \to K^0\pi^+$

$$\mathcal{B}(B^+ \to K^0\pi^+) = \begin{cases} |V_{tb}^*V_{ts}|^2|P_{K\pi}^{0+}|^2 & (\mathfrak{C}) \\ |V_{cb}^*V_{cs}|^2|P_{K\pi}^{0+}|^2 & (\mathfrak{T}) \end{cases} \tag{39}$$

(for the conventions $\mathfrak{C}$ and $\mathfrak{T}$, respectively, and where the doubly Cabibbo-suppressed u Penguin has been neglected and the identity $P(\mathfrak{C}) = P(\mathfrak{T})$ is used) by means of the relation [11]

$$|P^{+-}| \approx \frac{1}{\sqrt{r_\tau}} \frac{f_\pi}{f_K} \frac{1}{R_{\rm th}} |P_{K\pi}^{0+}| \ . \tag{40}$$

Neglecting SU(3) symmetry breaking, electroweak penguins and OZI-suppressed penguins as well as annihilation contributions, one finds that $|P^{+-}| = |P^{0+}_{K\pi}|$. The improvement of this approximation attempted in Eq. (40) corrects for the different lifetimes of charged and neutral B mesons, $r_\tau = \tau_{B^+}/\tau_{B^0} = 1.086 \pm 0.016$ [12], and for SU(3) breaking estimated within naive factorization (FA). This neglects strong rescattering amplitudes. The additional factor, $R_{\rm th} = 0.98 \pm 0.05$ [13], introduces an estimate of SU(3) breaking based on an improved QCD Factorization Approximation (see following section). One has to stress that no theoretical error on the various dynamical assumptions, such as the size of non-factorizable contributions, or the assumption that $B^+ \to K^0\pi^+$ is given by a pure penguin amplitude, is assigned here. Note that the strong phase $\delta_{\pi\pi}$ remains unconstrained in this method.

The size of the tree amplitude $|T^{+-}|$ is conveniently deduced from the measurement of $\mathcal{B}^{+-}$, taking advantage of the above estimate of $|P^{+-}|$. We thus assure the proper interpretation within the amplitude conventions $\mathfrak{U}$, $\mathfrak{C}$ or $\mathfrak{T}$ applied. Other methods to estimate the tree amplitude can be found in the literature:

1. one can use the spectrum of decay $B^0 \to \pi^+\ell^-\bar{\nu}$ near $q^2 = 0$ (the squared effective mass of the recoiling $\ell\nu$ system) in addition with theoretical estimates for the form factor [11], giving $R_u|T_u| = (2.7 \pm 0.6) \times 10^{-3}$; the method is not used here as it provides $|T_u|$ rather than the full $|T^{+-}|$.

2. according to Eqs. (27) and (31), the tree-only decay $B^+ \to \pi^+\pi^0$ is given by

$$\mathcal{B}^{\pm 0} = R_u^2 \left(\frac{1}{2}|T^{+-}|^2 + |T_C^{00}|^2 + \sqrt{2}{\rm Re}\left[T^{+-}T_C^{00*}\right]\right) . \qquad (41)$$

   Using theoretical assumptions on the ratio $|T_C^{00}/T^{+-}|$ one may infer the size of $|T^{+-}|$ from the measured branching ratio [11].

2.7 Beyond naive factorization

New theoretical efforts to calculate the tree and penguin amplitudes in $B \to hh'$ on the basis of QCD have been developed in recent years. If such calculations reliably predicted the penguin and tree diagrams and their relative strong phase difference, they could be used to translate a measurement of $S_{\pi\pi}$ and $C_{\pi\pi}$ into a powerful constraint on the CKM phase.

The QCD Factorization Approach (QCD FA) [13] is based on the concept of color transparency. In the heavy quark limit ($m_b \gg \Lambda_{\rm QCD}$), the decay amplitudes are calculated using a new factorization theorem. To leading power in $\Lambda_{\rm QCD}/m_b$ and in lowest order in perturbation theory, the result of naive factorization is reproduced. It is found that non-factorizable corrections are calculable as perturbative corrections in α_s since the interaction of soft gluons with the small color-dipole of the high-energetic quark-anti-quark pair is suppressed. Non-factorizable power-suppressed[6] contributions are not calculable

[6] The term "power suppression" refers to the quantity $\Lambda_{\rm QCD}/m_b \ll 1$.

ID	$\|T^{+-}\|$	$\arg(T^{+-})$	$\|P^{+-}\|$	$\arg(P^{+-})$	$\|T_C^{00}\|$	$\arg(T_C^{00})$	$P_{\rm EW}^{+0}$	$\arg(P_{\rm EW}^{+0})$
(A)	1	0	0	0	1/3	0	0	0
(B)	1	180°	0	0	1/3	0	0	0
(C)	1	0	1/4	0	1/3	0	0	0
(D)	1	0	1/2	0	1/3	0	0	0
(E)	1	0	1/2	180°	1/3	0	0	0
(F)	1	0	1/2	90°	1/3	0	0	0
(G)	1	0	0	0	1/3	0	1/4	90°
(H)	0.58	−40°	0.07	177°	0.20	−94°	0.11	−63°

Table 1: *Parameter settings for the exercises depicted in Figs. 6 and 7. The G setup includes the occurrence of electroweak penguins which are however restricted to the $\pi^+\pi^0$ and $\pi^0\pi^0$ modes only. The last line (H) corresponds to one of the infinite number of generating amplitudes that reproduce the central values of the measured branching fractions and CP asymmetries given in Table 2. Note that other solutions may significantly differ from the one chosen here.*

within this framework. Infrared endpoint singularities arise in the hard spectator interactions and in the annihilation diagrams which are estimated in a model-dependent way. These contributions are parameterized by two complex quantities, X_H and X_A, assumed to be small.

The penguin-to-tree ratio and the strong phase difference between the penguin and tree amplitudes are predicted with relatively small theoretical uncertainties. The dominant errors relevant for the theoretical prediction of $S_{\pi\pi}$ and $C_{\pi\pi}$ arise from the strange quark mass, gauging the size of so-called chirally enhanced penguins, from the charm quark mass, entering the calculation of penguins with a charm quark in the loop, and from the scale dependence in $\alpha_s(\mu)$. The QCD FA has been implemented in *CKMfitter*.

Another approach, denoted pQCD [14], differs from QCD FA mainly in the power counting in terms of $\Lambda_{\rm QCD}/m_b$. The pQCD approach is not yet implemented in *CKMfitter*.

There is an ongoing debate among the experts concerning the reliability of these calculations. The main concerns here are the computation of the chirally enhanced penguins, see, *e.g.*, Ref. [15], endpoint singularities in hard spectator interactions and the control of non-factorizable annihilation contributions.

3 Exercises

The purpose of this section is to illustrate the consequences of different sets of tree and penguin contributions and their phases to the physical observables measured by the ex-

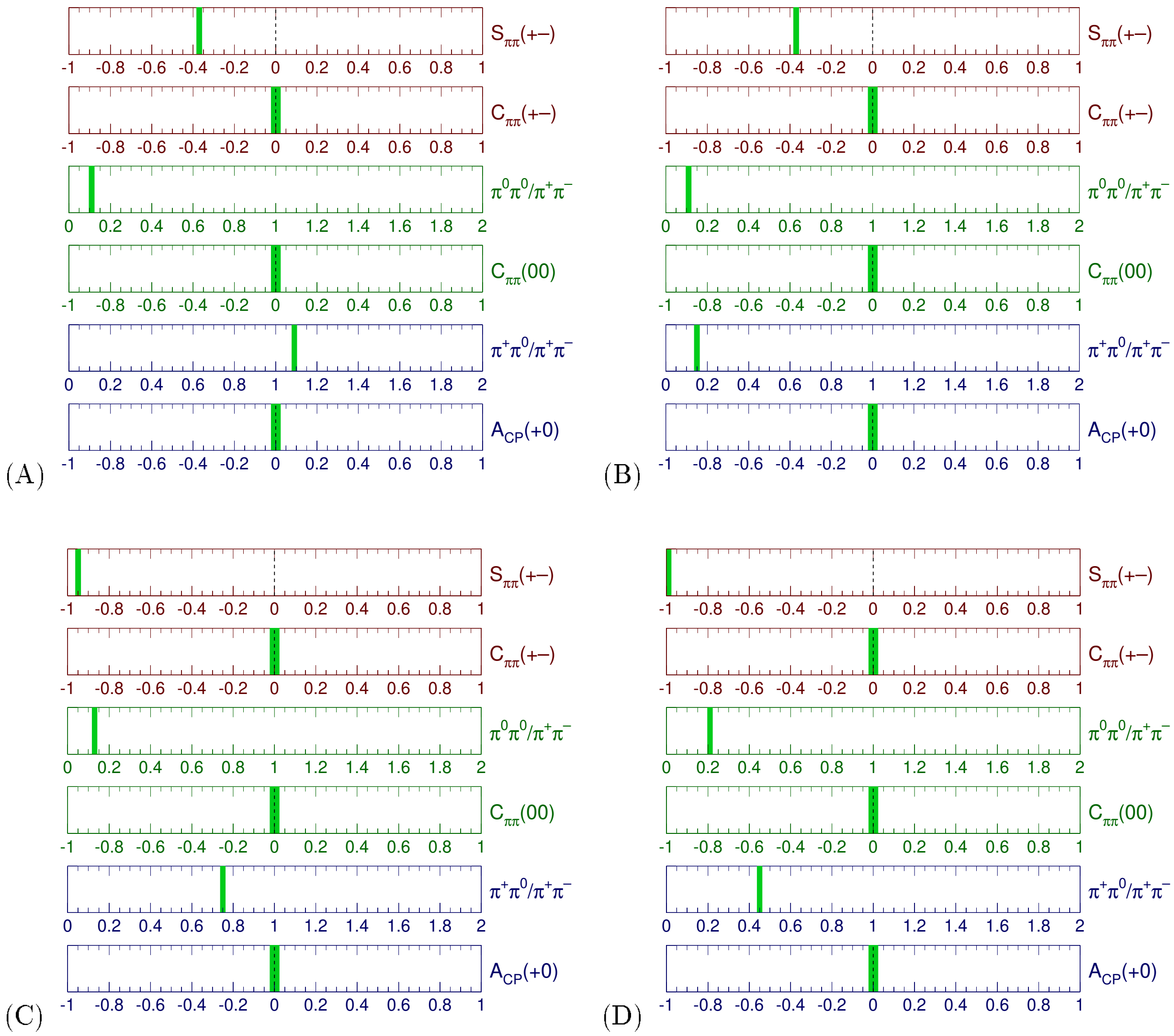

Figure 6: *Consequences of the settings (A-D)* (cf. *Table 1) for the tree and penguin amplitudes and their phases on the physical observables. The ratios* $\pi^{0(+)}\pi^0/\pi^+\pi^-$ *denote ratios of branching fractions.*

(A) Only the T^{+-} amplitude is present. As a consequence $S_{\pi\pi} = \sin 2\alpha = \sin(2\cdot 101^\circ) = -0.38$ and no direct CP violation is present. It is noticeable that $\mathcal{B}^{+0} \simeq \mathcal{B}^{+-}$.
(B) A strong T^{+-} phase of 180° does not affect the CP observables. However, it does lead to a reduction of $\mathcal{B}^{+0} \ll \mathcal{B}^{+-}$.
(C) The presence of penguins affects $S_{\pi\pi}$, which no longer corresponds to $\sin 2\alpha$, even if the relative strong phase vanishes. No direct CP violation is generated.
(D) An enhanced penguin contribution (here, one half of the size of the tree amplitude) leads to an increased $\mathcal{B}^{00}/\mathcal{B}^{+-}$ to the detriment of $\mathcal{B}^{+0}\mathcal{B}^{+-}$. Again, no direct CP violation is generated.

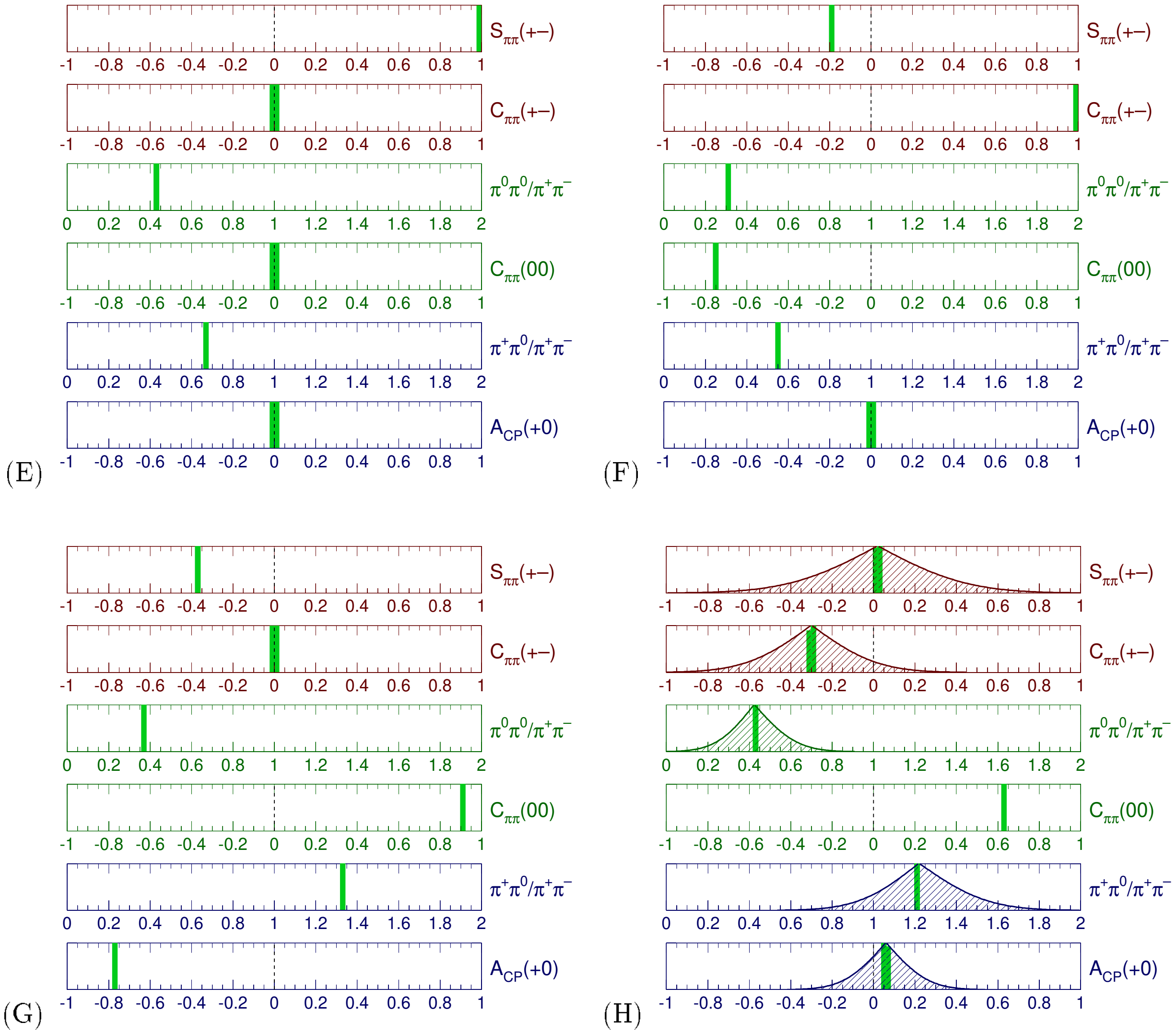

Figure 7: *Consequences of the settings (E-H)* (cf. *Table 1) for the tree and penguin amplitudes and their phases on the physical observables. The ratios $\pi^{0(+)}\pi^0/\pi^+\pi^-$ denote ratios of branching fractions.*

(E) A relative strong phase of 180° between T^{+-} and P^{+-} alters the sign of $S_{\pi\pi}$ but does not generate direct *CP* violation. The ratios $\mathcal{B}^{00}/\mathcal{B}^{+-}$ and $\mathcal{B}^{+0}\mathcal{B}^{+-}$ increase wrt. D.
(F) A relative strong phase of 90° between T^{+-} and P^{+-} affects $S_{\pi\pi}$ and generates direct *CP* violation $C_{\pi\pi} \neq 0$, $C_{\pi^0\pi^0} \neq 0$ (with opposite signs).
(G) This setup corresponds to (A), *i.e.*, no strong penguins are present, but it has a significant contribution from electroweak penguins, generating direct *CP* violation in $\pi^+\pi^0$ (charge asymmetry) and $\pi^0\pi^0$ (flavour asymmetry). EW penguins do not contribute to A^{+-} here.
(H) This is one solution of an infinite number of generating amplitudes that reproduce the central values of the measured branching fractions and *CP* asymmetries given in Table 2. Also shown are the confidence levels of the experimental values.

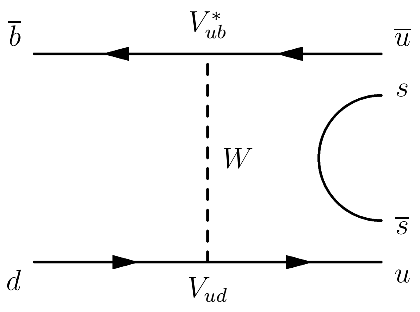

Figure 8: *W exchange diagram responsible for the decay $B^0 \to K^+K^-$.*

periments. If not stated otherwise, isospin invariance is assumed to hold during the following exercises. We chose as central values $\bar{\rho} = 0.24$ and $\bar{\eta} = 0.34$, corresponding to $\alpha = 101°$. Among the infinite sample size of interesting combinations, we have chosen the palette identified by the labels (A-H) in Table 1 and plotted in Figs. 6 and 7. They exhibit increasing complexity, leading to shifts in $S_{\pi\pi} \neq \sin 2\alpha$ and to direct *CP* violation ($C_{\pi\pi} \neq 0$, $C_{\pi^0\pi^0} \neq 0$ and/or $A_{\rm CP}^{+0} \neq 0$). According to Eqs. (19,20), direct *CP* violation requires either significant strong penguin contribution *and* a non-trivial relative strong phase between tree and penguins amplitude, or the presence of a significant electroweak penguin amplitude. This latter option is simulated in the setup G. For demonstration purposes we restrict however the occurrence of electroweak penguins to the $\pi^+\pi^0$ and $\pi^0\pi^0$ modes only, though in reality a significant contribution here could well lead to a similar enhancement in the penguin amplitude of $\pi^+\pi^-$ as well. The last setup (H) corresponds to one of the infinite number of generating amplitudes that reproduce the central values of the measured branching fractions and *CP* asymmetries given in Table 2. Of course, other solutions may strongly differ from the one chosen here.

4 The Input Data

A compilation of branching fractions and charge asymmetries (direct *CP* violation) of all $B \to hh'$ modes ($hh' = \pi, K$) is given in Table 2. We compute the world averages, taking into account asymmetric errors and assuming the individual positive and negative pieces of the likelihoods to be Gaussian. The subsequent fits will use the same assumption. At present, common systematic errors affecting the measurements, such as the total number of B's produced, their relative charged and neutral fractions, efficiencies of photon and track reconstruction, are not taken into account. However, with increasing statistics they will become important and shall be incorporated. Most of the rare, two-body pseudoscalar decay modes are discovered. The missing modes have either color-suppressed trees only ($\mathcal{B}^{00}$), or are mediated via power-suppressed W exchange/annihilation diagrams ($B^0 \to K^+K^-$, see Fig. 8) and hence are expected to be small. We use the most restrictive 90% CL limits for these. No significant charge asymmetry has been observed so far. Note that non-zero direct *CP* asymmetry measured in $B^+ \to \pi^+\pi^0$ would indicate

Mode	*BABAR*	Belle	CLEO	World average
$B^0 \to \pi^+\pi^-$	$4.7 \pm 0.6 \pm 0.2$ [16]	$5.4 \pm 1.2 \pm 0.5$ [22]	$4.3^{+1.6}_{-1.4} \pm 0.5$ [24]	4.78 ± 0.54
$B^+ \to \pi^+\pi^0$	$5.5^{+1.0}_{-0.9} \pm 0.6$ [18]	$7.4^{+2.3}_{-2.2} \pm 0.9$ [22]	$5.6^{+2.1}_{-2.0} \pm 1.5$ [24]	5.83 ± 0.96
$B^0 \to \pi^0\pi^0$	< 3.6 [19] $(1.6^{+0.7}_{-0.6}{}^{+0.6}_{-0.3})$	< 6.4 [22] $(3.2 \pm 1.5 \pm 0.7)$	< 5.7 [25] $(2.2^{+1.7}_{-1.3} \pm 0.7)$	$2.01^{+0.70}_{-0.67}$
$B^0 \to K^+\pi^-$	$17.9 \pm 0.9 \pm 0.7$ [16]	$22.5 \pm 1.9 \pm 1.8$ [22]	$17.2^{+2.5}_{-2.4} \pm 1.2$ [24]	18.46 ± 0.98
$B^+ \to K^+\pi^0$	$12.8^{+1.2}_{-1.1} \pm 1.0$ [18]	$13.0^{+2.5}_{-2.4} \pm 1.3$ [22]	$11.6^{+3.0}_{-2.7}{}^{+1.4}_{-1.3}$ [24]	12.68 ± 1.23
$B^+ \to K^0\pi^+$	$17.5^{+1.8}_{-1.7} \pm 1.3$ [20]	$19.4^{+3.1}_{-3.0} \pm 1.6$ [22]	$18.2^{+4.6}_{-4.0} \pm 1.6$ [24]	$18.09^{+1.73}_{-1.69}$
$B^0 \to K^0\pi^0$	$10.4 \pm 1.5 \pm 0.8$ [18]	$8.0^{+3.3}_{-3.1} \pm 1.6$ [22]	$14.6^{+5.9}_{-5.1}{}^{+2.4}_{-3.3}$ [24]	10.34 ± 1.48
$B^0 \to K^+K^-$	< 0.6 [16]	< 0.9 [22]	< 1.9 [24]	
$B^+ \to K^+\overline{K}^0$	< 1.3 [20]	< 2.0 [22]	< 5.1 [24]	
$B^0 \to K^0\overline{K}^0$	< 7.3 [21]	< 4.1 [22]	$-$	
$A_{CP}(\pi^+\pi^0)$	$-0.03^{+0.18}_{-0.17} \pm 0.02$ [18]	$+0.30 \pm 0.30^{+0.06}_{-0.04}$ [22]	-	$+0.06 \pm 0.16$
$A_{CP}(K^+\pi^-)$	$-0.102 \pm 0.050 \pm 0.016$ [16]	$-0.07 \pm 0.06 \pm 0.01$ [23]	-0.04 ± 0.16 [26]	-0.086 ± 0.039
$A_{CP}(K^+\pi^0)$	$-0.09 \pm 0.09 \pm 0.01$ [18]	$-0.02 \pm 0.19 \pm 0.02$ [22]	-0.29 ± 0.23 [26]	-0.101 ± 0.077
$A_{CP}(K^0\pi^+)$	$-0.17 \pm 0.10 \pm 0.02$ [20]	$+0.02 \pm 0.09 \pm 0.01$ [23]	$+0.18 \pm 0.24$ [26]	-0.05 ± 0.07
$A_{CP}(K^0\pi^0)$	$0.03 \pm 0.36 \pm 0.09$ [18]	-	-	0.03 ± 0.37

Table 2: *Compilation of results (status ICHEP 2002) on $B \to hh'$ branching fractions (in units of 10^{-6}) and direct* CP *asymmetries. Limits are quoted at 90% CL. The world averages are computed taking into account asymmetric errors. See text for more information.*

a contribution from electroweak penguins (since annihilation is in weak phase with the dominant tree amplitude).

We use the results on time-dependent *CP* asymmetry measured by *BABAR* [16] and Belle [17] (statistical and systematic errors have been added in quadrature):

	$S_{\pi\pi}$	$C_{\pi\pi}$	ρ
BABAR	0.02 ± 0.34	-0.30 ± 0.25	-0.10
Belle	$-1.21\,^{+0.41}_{-0.30}$	$-0.94\,^{+0.32}_{-0.27}$	0.28
Average	-0.48 ± 0.26	-0.54 ± 0.20	0.09
χ^2	$5.3 \to 2.2\sigma$	$2.2 \to 1.5\sigma$	

(42)

where we have reversed the sign of Belle's $C_{\pi\pi} = -A_{\pi\pi}$ to account for the different convention adopted. The last column in Eq. (42) gives the statistical correlation coefficients between $S_{\pi\pi}$ and $C_{\pi\pi}$ as quoted by the experiments. If not stated otherwise we do not use the averages but rather the *BABAR* results in the following studies.

5 Numerical Analysis of $B \to hh'$ Decays

We are running *CKMfitter* corresponding to the analysis stages (I) through (IV), using the inputs from Table 2. All plots have been produced using the *BABAR* measurement for $S_{\pi\pi}$ and $C_{\pi\pi}$. The constraints are shown in Figs. 9 and 10 for the $(\bar\rho, \bar\eta)$ plane and α, respectively.

- Due to the large upper limit for $\mathcal{B}^{00}$, potentially caused by the presence of a signal, there are essentially no constraints from the SU(2) analysis, stage I(upper left hand plot). We find the limit $|\theta| < 51^\circ$ at 90% CL.

- Using in addition SU(3) (stage II) one begins to weakly rule out regions in the $(\bar\rho, \bar\eta)$ plane (upper right hand plot). The wide unconstrained arcs correspond to the still unfruitful bound $|\theta| < 29^\circ$ at 90% CL. These constraints cannot compete with the size of the allowed $(\bar\rho, \bar\eta)$ region obtained from the standard CKM fit.

- Non-trivial information can be obtained when strategy (III) is used to constrain $|\theta|$ (lower left hand plot). We find the limit $|\theta| < 20^\circ$ at 90% CL. Nevertheless, even with much larger statistics the accuracy of the constraint will not outperform the present standard CKM fit (*cf.* comments in Section 2.6). The reason for this is that these methods only provide information on the absolute size of the penguin pollution, without however determining the relative strong phase. Also, no theoretical errors have been assigned here with respect to the dynamical assumptions made.

- Only when using the highly predictive QCD FA (IV) for $|P^{+-}/T^{+-}|$ and $\delta_{\pi\pi}$ relatively stringent constraints in the $(\bar\rho, \bar\eta)$ plane are obtained, which with present statistics are already competitive with those obtained from the standard CKM fit. Indeed, taking into account all theoretical uncertainties as quoted by the authors [13], the resulting precision is experimentally (statistically) limited. The preferred region in the $(\bar{\rho}, \bar{\eta})$ plane within the QCD FA is found at negative values for $\bar{\eta}$ due to the negative central value of $C_{\pi\pi}$ measured by *BABAR* and the small predicted values for $\delta_{\pi\pi}$ (*cf.* Section 2.2). However, since the measurement is not yet significant, the constraints from $S_{\pi\pi}$ and $C_{\pi\pi}$ within the QCD FA are found in comfortable agreement with those obtained from the standard CKM fit.

The predictions obtained for $S_{\pi\pi}$ and $C_{\pi\pi}$ for the analysis steps (I) through (IV) are depicted in Fig. 11. An input requirement to these predictions is the value of the CKM phase. It is therefore assumed in this exercise that the Standard Model is correct so that $\bar{\rho}$ and $\bar{\eta}$ can be constrained by means of the standard CKM fit (see Appendix B), the errors of which are properly propagated in the calculations. As a result, it is found that, in accordance with what has been said above, the present experimental input used in the SU(2) analysis (I) is not able to constrain $S_{\pi\pi}$ and $C_{\pi\pi}$ due to the weak bound on $\mathcal{B}^{00}$. Again, little information is obtained from the SU(3) analysis (II) and strategy (III), while the QCD FA (IV) remains predictive. The relatively large uncertainty in $S_{\pi\pi}$ is due to the weak $\sin 2\alpha$ constraint of the standard CKM fit. Values for $C_{\pi\pi}$ that are far from zero, as suggested by the Belle measurement, cannot be reproduced by the QCD FA since the strong phase difference $\delta_{\pi\pi}$ is predicted to be small. In turn, were such large values for $C_{\pi\pi}$ correct, would be a strong hint for a large phase difference $\delta_{\pi\pi}$, since it is unlikely that large direct *CP* violation can arise from new physics contributions alone[7]. Negative values for $C_{\pi\pi}$, even if they are small, are disfavoured by the QCD FA so that the forthcoming experimental updates are anxiously expected.

One can revert the point-of-view and constrain the QCD unknowns, penguin-to-tree ratio r^{+-} (10) and its phase, instead of the CKM parameters. Again, this assumes that the measurements of $S_{\pi\pi}$ and $C_{\pi\pi}$ are in agreement with the constraints obtained on $\bar{\rho}$ and $\bar{\eta}$ in the standard CKM fit, *i.e.*, no new physics comes into play. The resulting confidence levels are shown in Fig. 12 for the two conventions $\mathfrak{C}$ and $\mathfrak{T}$. The preferred values for r^{+-} are in agreement with those obtained from naive factorization [11] or QCD FA (IV). Since the standard CKM fit constraints $\bar{\eta}$ to be positive (and thus $\gamma > 0$), the preferred values for $\delta_{\pi\pi}$ are negative.

In Fig. 13, we give the constraints on the branching fraction $\mathcal{B}^{00}$ using the experimental information from $\mathcal{B}^{+-}$, $\mathcal{B}^{\pm 0}$ and $C_{\pi\pi}$ (see also Eq. (35)) where the *BABAR* and Belle results for $C_{\pi\pi}$ have been treated separately. One observes that the lower limit on $\mathcal{B}^{00}$ becomes interesting for very large values of $|C_{\pi\pi}|$. In effect, if $C_{\pi\pi}$ were the value measured by Belle, it could already set significant constraints on theoretical calculations, without a direct measurement of $\mathcal{B}^{00}$, and only due to the constraints from the isospin relations.

[7]This can be seen as follows: if the relative strong phase is small, an additional contribution from new physics with phase that alters its sign under *CP* conjugation (like the weak phase) would only create direct *CP* violation if the new physics were accompanied by a large strong phase. The QCD piece would then differ from that of the Standard Model contributions, which deems unlikely to us.

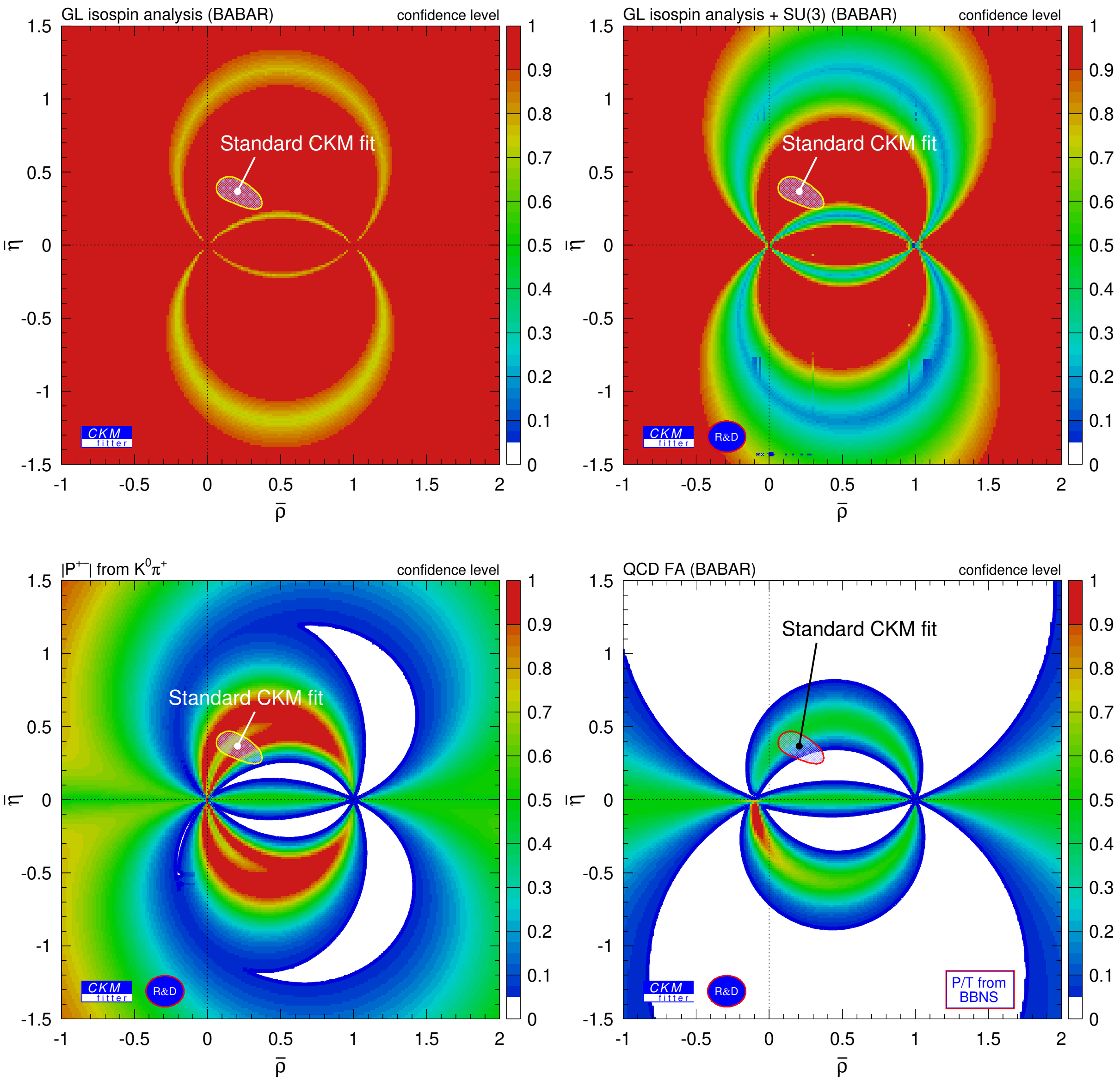

Figure 9: *Confidence levels in the* $(\bar{\rho}, \bar{\eta})$ *plane for the analysis steps (I) through (IV)* (cf. *Section 1). Overlaid on each plot is the prediction from the standard CKM fit which includes the world average of* $\sin 2\beta$*. Significant constraints are obtained once the penguin-to-tree ratio is determined using theoretical or phenomenological input (steps (III) and (IV)). Consistency with the Standard Model is found. Due to the negative value of* $C_{\pi\pi}$*, the* $\bar{\eta} < 0$ *half plane is favoured in the QCD FA (lower right hand plot). Without predicting the relative strong phase, the sign information on* $\bar{\eta}$ *from the measurement of direct CP violation cannot be exploited. The plots corresponding to analysis steps (I) through (III) are thus symmetric with respect to* $\pm\bar{\eta}$*. The comparison of the allowed regions obtained in (IV) (phases and magnitude of the tree and penguin amplitudes are predicted and their uncertainties are small with respect to the experimental errors) shows that the experimental accuracy is already competitive with the standard CKM constraint.*

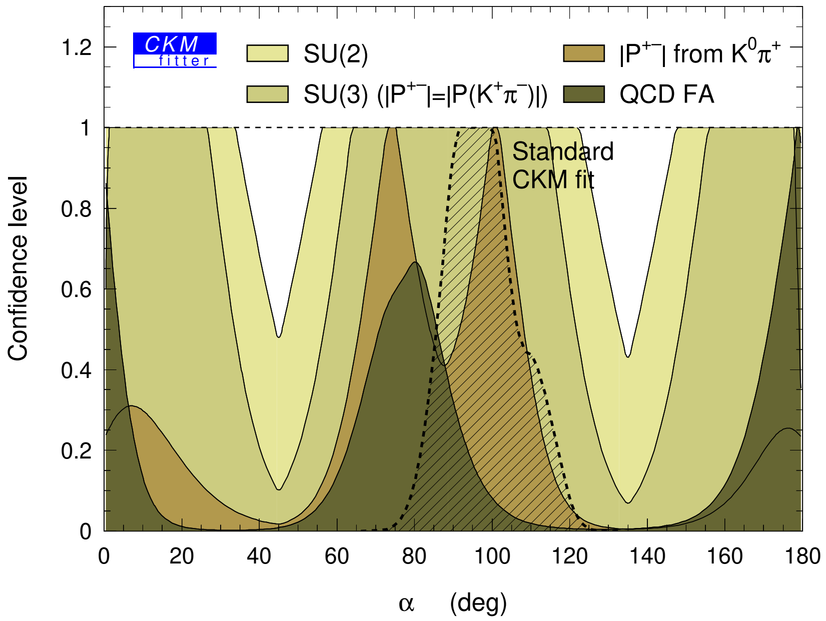

Figure 10: *Confidence levels in α for the analysis steps (I) through (IV) and using CP and branching fraction results of $B \to hh'$ decays. The radius $(\bar{\rho}^2 + \bar{\eta}^2)^{1/2}$ has been confined using in addition $|V_{ub}|$. Overlaid (dashed line, hatched area) is the prediction from the standard SM fit which includes the world average of $\sin 2\beta$. Significant constraints (up to the four-fold ambiguity) are obtained once the penguin-to-tree ratio is determined (steps (III) and (IV)). Consistency with the Standard Model and comparable uncertainties are found for these cases.*

For example, QCD FA predicts $\mathcal{B}^{00}$ in the range $0.1 - 3.3 \cdot 10^{-6}$ (*cf.*, the hatched area in Fig. 13), where larger values branching fractions correspond to larger values of γ. We presume that the larger errors found here with respect to Fig. 13 in Ref. [13] is due to differences in the treatment of the theoretical uncertainties.

6 Prospects

The preceding sections have shown that, at present, relevant information on α can be only inferred if substantial theoretical input is used to predict the size of the penguin contribution. However, the ultimate goal of the experimental effort should be the unequivocal determination of α without relying on model dependent theoretical descriptions.

This prejudice given, we shall return to the full isospin analysis, *i.e.*, we assume the B^0-flavour in $B^0 \to \pi^0\pi^0$ is tagged, to dare an outlook into the future. Notwithstanding keeping in mind that we neglect electroweak penguin amplitudes the presence of which would lead to shifts in angles and sides of the isospin triangles (see Fig. 4).

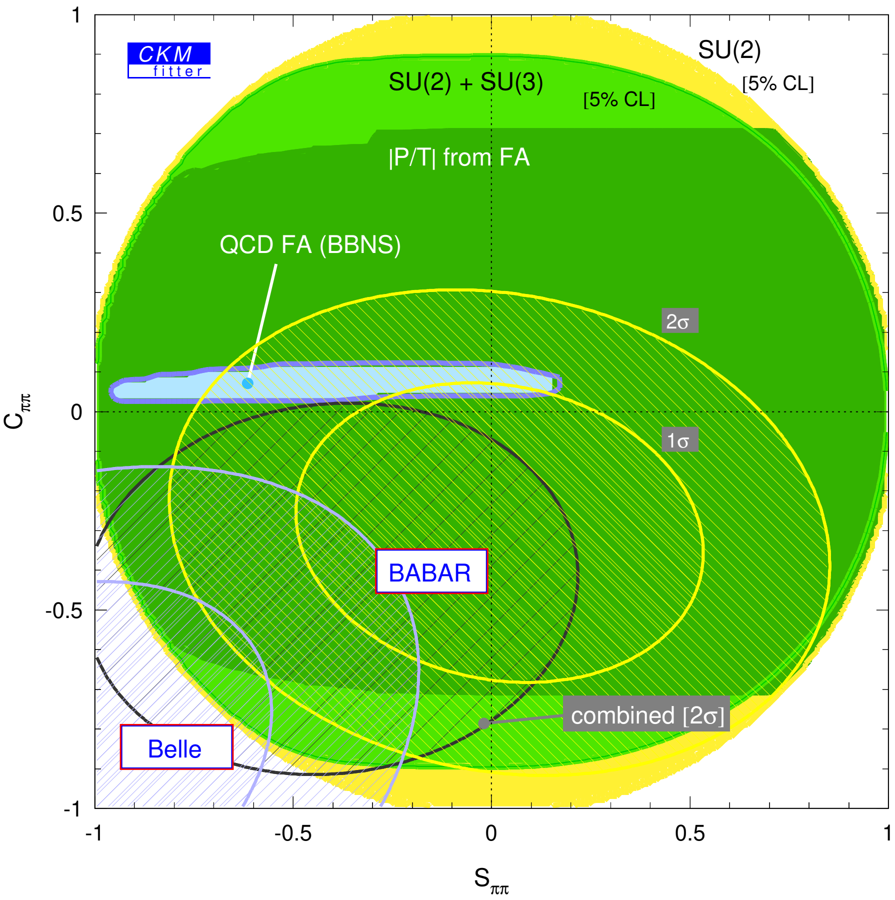

Figure 11: *Predictions for $S_{\pi\pi}$ and $C_{\pi\pi}$ for the analysis steps (I) through (IV). The input values for $\bar{\rho}$ and $\bar{\eta}$ are taken from the standard CKM fit assuming the Standard Model to hold. The relatively large uncertainty of the QCD FA in $S_{\pi\pi}$ is due to the weak* $\sin 2\alpha$ *constraint of the standard CKM fit. For comparison, the 1 σ and 2 σ contours for the experimental results from BABAR, Belle and their avaerage have been overlaid.*

Figure 14 shows the residual θ for the present (ICHEP'02) central values of the $B \to \pi\pi$ branching fractions (*cf.* Table 2). For $S_{\pi\pi}$ and $C_{\pi\pi}$ the central values of the *BABAR* measurement have been used. Distinguished are four cases: (i) the current statistics (but assuming the individual rates $B^0(\overline{B}^0) \to \pi^0\pi^0$ have been measured, see below), (ii) a luminosity of 500 fb^{-1} reached by *BABAR* in a few years from now, (iii) hypothetical 2000 fb^{-1} reached by the first generation B-factories at the end of their running period and, (iv), 10000 fb^{-1} collected by a second generation B factory after a few years of running. Note that the central values are kept unchanged in all cases. The full isospin analysis is employed, *i.e.*, we assume the flavours of $B^0(\overline{B}^0) \to \pi^0\pi^0$ are tagged. Moreover, we assume that direct CPV is absent ($|\lambda_{\pi^0\pi^0}| = 1$) leading to the symmetric solutions shown in Fig. 14. Mistag rates and the dilution from the time-integrated measurement have been taken into account in the extrapolation. For missing $B^0 \to \pi^0\pi^0$ flavour information (as

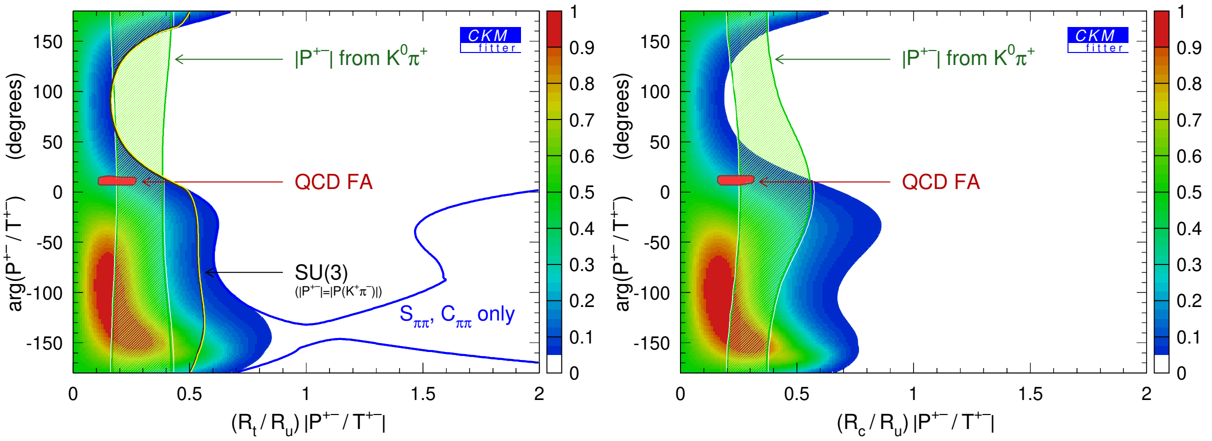

Figure 12: *Constraints on the penguin-to-tree ratio r^{+-} and the relative strong phase $\delta_{\pi\pi}$. The shaded (coloured) region gives the confidence levels obtained from a fit corresponding to the approach (I) (SU(2), cf. introduction). The CKM phase is constrained by means of the standard CKM fit. The extended contour indicates the 5% CL limit when only using $S_{\pi\pi}$ and $C_{\pi\pi}$. Also shown are the 5% CL contours corresponding to the approaches (II) (SU(3)), (III) ($|\boldsymbol{P^{+-}}|$ from $\boldsymbol{B^+ \to K^0\pi^+}$) and (IV) (QCD FA). Left hand plot: convention $\mathfrak{C}$; Right hand plot: convention $\mathfrak{T}$.*

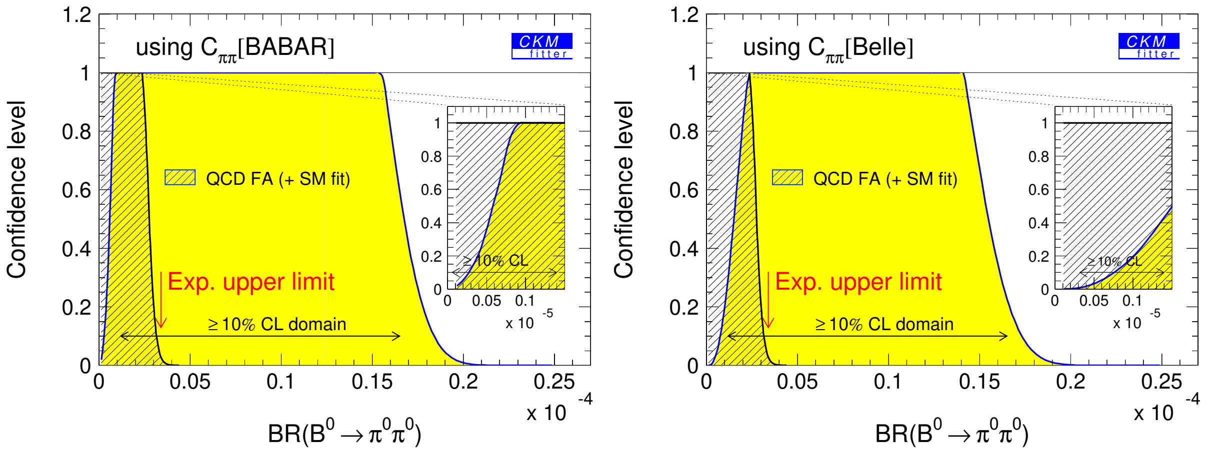

Figure 13: *Constraint on the branching fraction $\mathcal{B}^{00}$ obtained from the measurements of $\mathcal{B}^{+-}$, $\mathcal{B}^{\pm 0}$ and $C_{\pi\pi}$ using the isospin relations (26). This is equivalent to using Eq. (35). Given by the hatched area is the prediction from QCD FA [13]: larger $\mathcal{B}^{00}$ branching fractions require larger values of the UT angle γ. Left: using $C_{\pi\pi}$ from BABAR, and right from Belle, respectively. The vertical arrow indicates the experimental upper limit at 90% CL found by BABAR. The horizontal arrows indicate the zone for which the CL is equal or better than 10%.*

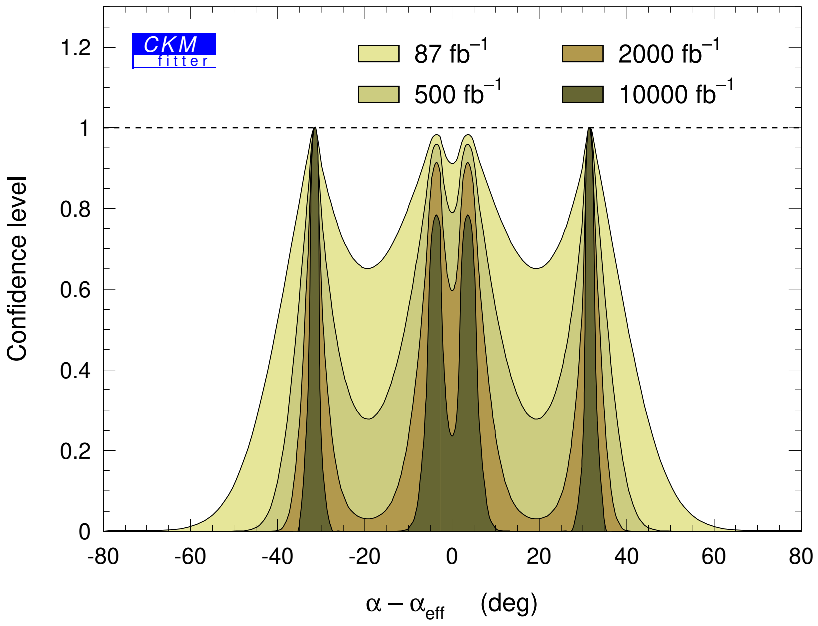

Figure 14: *The residual $\alpha - \alpha_{\rm eff}$ for the present (ICHEP'02) central values (see Table 2) and errors as well as projected luminosities of BABAR, Belle and future B-factories (always keeping the central values unchanged). Note that due to finite binning only, the central peaks do not reach until $CL = 1$. The full isospin analysis is employed, i.e., we assume the flavours of $B^0(\overline{B}^0) \to \pi^0\pi^0$ are tagged. Moreover, we assume that direct CPV is absent ($|\lambda_{\pi^0\pi^0}| = 1$) leading to the symmetric solutions shown in the figure). When the flavour information for $B^0 \to \pi^0\pi^0$ is missing (as currently the case), only the outer borders of the curves can be obtained from the isospin analysis Eqs. (33-34), while the inner structure remains unresolved because the strong phase of the tree amplitude is unconstrained. The inner structure reveals the remnants of the eight-fold ambiguity in the range $\alpha \in \{0, 2\pi\}$. For this setup of central values, only luminosities of the order of* 10 ab^{-1} *allow to separate the solutions.*

currently the case), only the outer borders of the curves can be obtained from the isospin analysis Eqs. (33-34), while the inner structure remains unresolved because the relative strong phase is unconstrained. The inner structure reveals the remnants of the eight-fold ambiguity the full isospin analysis in the range $\alpha \in \{0, 2\pi\}$. For this setup of central values, only luminosities of the order of 10 ab^{-1} allow to separate the solutions. Without a separation, the overall allowed region exceeds the uncertainty of the SM fit (*cf.* Fig. 10).

For a detailed analysis on using the Grossman-Quinn bound in various long-term scenarios and $B^0 \to \pi^0\pi^0$ branching ratios, see Adrian Bevan's study in [27].

7 Conclusion

We have studied various strategies proposed in the literature to interpret the time-dependent asymmetry measured in $B^0 \to \pi^+\pi^-$ decays in terms of CKM parameters. The common goal of these strategies is to bound or determine the penguin contribution to the transition amplitude, using more or less theoretical or phenomenological input.

At present, significant constraints on the penguin pollution are only provided by theoretical calculations predicting the complex value of P^{+-}/T^{+-} such as QCD FA or pQCD. However, there is not yet agreement among theorists whether these calculations have control over all relevant theoretical assumptions made therein. In addition, a confrontation with experimental data of better statistics is still to come.

Estimating $|P^{+-}|$ from $B^+ \to K^0\pi^+$ provides a qualitative interpretation. It can also be useful to detect obvious inconsistencies with the phenomenological picture of $B \to \pi\pi$ decays. In this approach, we find for the difference between the experimental observable $\alpha_{\rm eff}$ and the UT angle α: $|\alpha - \alpha_{\rm eff}| < 20°$ at 90% CL.

The SU(2) bounds do not lead to useful constraints on $|\alpha - \alpha_{\rm eff}|$ ($\leq 51°$ at 90% CL), since the upper limit on $\mathcal{B}^{00}$ is rather large. Not very well-known is the fact that a much better penguin bound is obtained from a strategy proposed by Charles, who uses the branching fraction of the penguin-dominated $B^0 \to K^+\pi^-$ and assumes SU(3) as well as weak additional theoretical presumptions. Unfortunately, also in this case the constraint on $|\alpha - \alpha_{\rm eff}| \leq 29°$ (at 90% CL) is not stringent enough to allow to significantly measure α. In addition, since the relevant branching ratios are already measured with quite good precision, this bound is not expected to improve with more data. Only large values for $|C_{\pi\pi}|$ would improve the penguin bounds for both strategies, SU(2) and SU(3).

The present experimental information on $\mathcal{B}^{00}$ is compatible with a branching ratio of the order $(1-2)\cdot 10^{-6}$. In this case, it would be possible to perform the full isospin analysis as proposed by Gronau and London and to extract the penguin contribution from data. However, to constrain $|\alpha - \alpha_{\rm eff}|$ with good precision and to separate the ambiguities would require an integrated luminosity of $\sim 10\ {\rm ab}^{-1}$.

A Isospin

We recall the SU(2) amplitude decomposition for decays of $\boldsymbol{B}$ mesons into two isovectors, denoted $\boldsymbol{p}$ and $\boldsymbol{q}$. They belong to the iso-multiplet:

$$\left\{\begin{array}{l} p^+q^- \\ p^-q^+ \\ p^+q^0 \\ p^0q^+ \\ p^-q^0 \\ p^0q^- \\ p^0q^0 \end{array}\right. \tag{43}$$

We consider the matrix elements

$$< p, q|H_s|u\overline{u}\overline{d}, d > \quad , \tag{44}$$

for the decay of the $\boldsymbol{B^0}$, and

$$< p, q|H_s|u\overline{u}\overline{d}, u > \quad , \tag{45}$$

for the decay of the $\boldsymbol{B^+}$, respectively, where $\boldsymbol{H_s}$ denotes the strong Hamiltonian. The *CP* conjugated modes are written accordingly.

Example decomposition of the amplitude $\mathcal{A}^{+-}$ for the decay $B^0 \to p^+q^-$: the amplitude consists of a |ket>, representing the four quarks state emitted from the $\boldsymbol{B}$ meson, and of a <bra| which is the final state:

$$\mathcal{A}^{+-} = \ < p^+, q^-|H_s|u\overline{u}\overline{d}, d > \ . \tag{46}$$

In terms of isospin quantum numbers Eq. (46) reads

$$\begin{aligned} \mathcal{A}^{+-} \ = \ & \underbrace{< 1, 1|}_{(a)} \otimes \underbrace{< 1, -1|}_{(b)} H_s \underbrace{|3/2, 1/2 >}_{(c)} \otimes \underbrace{|1/2, -1/2 >}_{(d)} \\ & + \ < 1, 1| \otimes < 1, -1| H_s |1/2, 1/2 > \otimes |1/2, -1/2 > \end{aligned} \tag{47}$$

where (a) is $< I, I_3|$ related to p^+, (b) to p^-, (c) is $|I, I_3 >$ related to the system $u\overline{u}\overline{d}$ and (d) to the quark $\boldsymbol{d}$.
Labelling the amplitudes by the change in isospin ΔI in the $\boldsymbol{b}$-quark decay and by the isospin I_f of the final state, $A_{\Delta I, I_f} \equiv < I_f, I_{f,3}|H_s|I_i, I_{i,3} >_{\Delta I}$, and obtain from the Clebsch-Gordan coefficients:

$$\begin{aligned} \mathcal{A}^{+-} \ = \ & \left(\frac{1}{\sqrt{6}} < 2,0| + \frac{1}{\sqrt{2}} < 1,0| + \frac{1}{\sqrt{3}} < 0,0|\right) H_s \left(\frac{1}{\sqrt{2}}|2,0>_{3/2} + \frac{1}{\sqrt{2}}|1,0>_{3/2}\right) \\ & + \left(\frac{1}{\sqrt{6}} < 2,0| + \frac{1}{\sqrt{2}} < 1,0| + \frac{1}{\sqrt{3}} < 0,0|\right) H_s \left(\frac{1}{\sqrt{2}}|1,0>_{1/2} + \frac{1}{\sqrt{2}}|0,0>_{1/2}\right) \end{aligned}$$

$$
\begin{aligned}
&= \frac{1}{2\sqrt{3}} < 2,0|H_s|2,0>_{3/2} + \frac{1}{2} < 1,0|H_s|1,0>_{3/2} \\
&\quad + \frac{1}{2} < 1,0|H_s|1,0>_{1/2} + \frac{1}{\sqrt{6}} < 0,0|H_s|0,0>_{1/2} \\
&= \frac{1}{2\sqrt{3}} A_{3/2,2} + \frac{1}{2} A_{3/2,1} + \frac{1}{2} A_{1/2,1} + \frac{1}{\sqrt{6}} A_{1/2,0} \ ,
\end{aligned} \tag{48}
$$

where in the second step we have explicitly used the fact that H_s conserves isospin.

A.1 Results for the general case

Doing the same for the five amplitudes we are interested in, one obtains :

$$\mathcal{A}^{+-} = \frac{1}{2}\frac{1}{\sqrt{3}} A_{3/2,2} - \frac{1}{2} A_{3/2,1} + \frac{1}{2} A_{1/2,1} - \frac{1}{\sqrt{6}} A_{1/2,0} \ , \tag{49}$$

$$\mathcal{A}^{-+} = \frac{1}{2}\frac{1}{\sqrt{3}} A_{3/2,2} + \frac{1}{2} A_{3/2,1} - \frac{1}{2} A_{1/2,1} - \frac{1}{\sqrt{6}} A_{1/2,0} \ , \tag{50}$$

$$\mathcal{A}^{+0} = \frac{1}{2}\sqrt{\frac{3}{2}} A_{3/2,2} - \frac{1}{2}\frac{1}{\sqrt{2}} A_{3/2,1} + \frac{1}{\sqrt{2}} A_{1/2,1} \ , \tag{51}$$

$$\mathcal{A}^{0+} = \frac{1}{2}\sqrt{\frac{3}{2}} A_{3/2,2} + \frac{1}{2}\frac{1}{\sqrt{2}} A_{3/2,1} - \frac{1}{\sqrt{2}} A_{1/2,1} \ , \tag{52}$$

$$\mathcal{A}^{00} = \frac{1}{\sqrt{3}} A_{3/2,2} + \frac{1}{\sqrt{6}} A_{1/2,0} \ . \tag{53}$$

Since there exist five decay amplitudes but only four isospin amplitudes, one can relate the decay amplitudes to each other leading to a pentagonal relation

$$\sqrt{2}(\mathcal{A}^{+0} + \mathcal{A}^{0+}) = 2\mathcal{A}^{00} + \mathcal{A}^{+-} + \mathcal{A}^{-+} \ . \tag{54}$$

This relation holds for tree and penguin amplitudes separately.

A.2 Penguin amplitudes

Since gluons decay with $\Delta I = 0$, so that strong penguins cannot mediate $\Delta I = 3/2$ transitions, one is left with only two independent penguin contributions

$$\mathcal{P}^{+0} = -\mathcal{P}^{0+} = \frac{1}{\sqrt{2}}(\mathcal{P}^{+-} - \mathcal{P}^{-+}) \ , \tag{55}$$

$$\mathcal{P}^{00} = -\frac{1}{2}(\mathcal{P}^{+-} + \mathcal{P}^{-+}) \ . \tag{56}$$

A.3 $B \to \pi\pi$

In the specific case where $p = q = \pi$, since the wave function of the two identical bosons must be symmetric, only those amplitudes with even I are non zero. The total amplitudes A^{+-} and A^{+0} are defined by:

$$A^{+-} = \frac{1}{\sqrt{2}}(\mathcal{A}^{+-} + \mathcal{A}^{-+}) \quad \text{and} \quad \mathrm{A}^{+0} = \frac{1}{\sqrt{2}}(\mathcal{A}^{+0} + \mathcal{A}^{0+}) \ , \tag{57}$$

Equation (54) then simplifies to the triangle relation

$$\frac{1}{\sqrt{2}}A^{+-} + A^{00} \ = \ A^{+0} \ , \tag{58}$$

in general and we obtain for the penguins

$$P^{0+} \ = \ P^{+0} = 0 \ , \tag{59}$$

$$P^{00} \ = \ -\frac{1}{\sqrt{2}}P^{+-} \ . \tag{60}$$

Conclusion: there are no strong penguins in $\pi^+\pi^0$.

B The Standard CKM Analysis

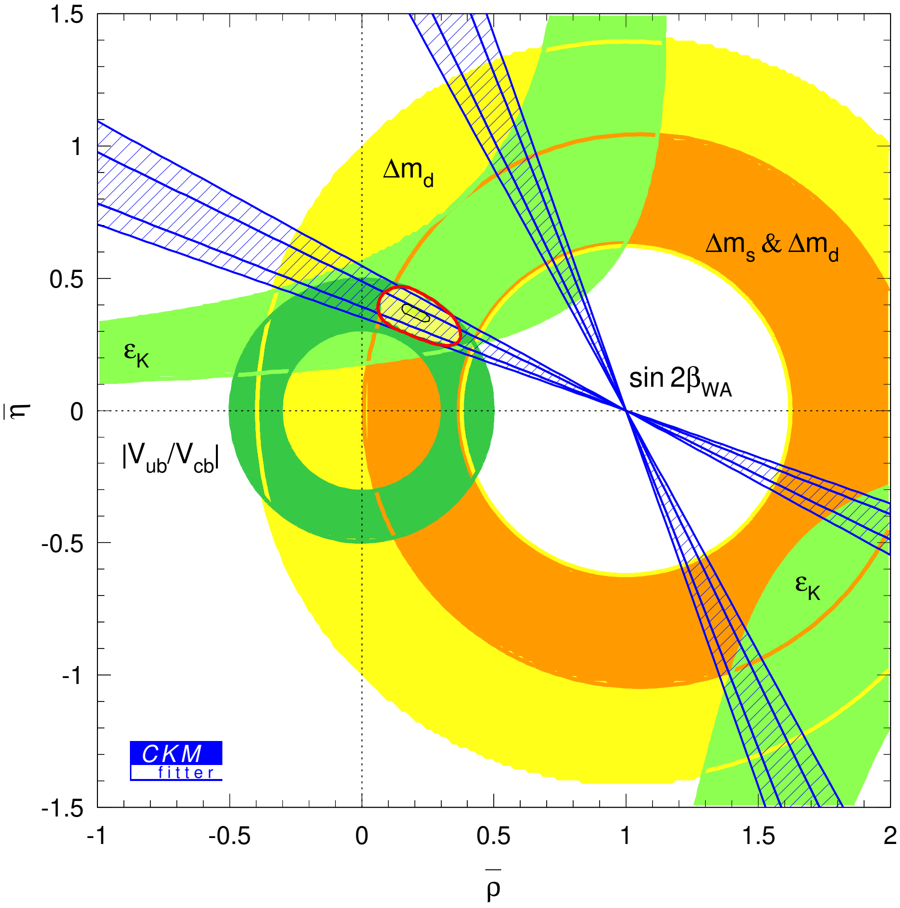

Figure 15: *Confidence levels in the enlarged* $(\bar{\rho}, \bar{\eta})$ *plane for the global CKM fit. The shaded areas indicate the regions of* $\geq$ **90%** *and* $\geq$ **5%** *CLs, respectively. Also shown are the* $\geq$ **5%** *CL domains of the individual constraints. The* $\geq$ **32%** *and* $\geq$ **5%** *CL constraints from the world average of the* $\sin 2\beta$ *measurements, entering the combined fit, are depicted by the dashed areas. See Table 3 for a compendium of the fit input values. All four ambiguities are drawn, three of which are excluded by the Standard Model.*

In several applications discussed in this note we relate the results obtained in the various $B \to hh'$ analyses to the constraints on the CP-violating CKM phase from the standard CKM analysis [1]. The standard analysis uses results on mixing and CP violation from the K^0 and B^0 systems as well as the direct measurements of the CKM matrix elements $|V_{ud}|$, $|V_{us}|$, $|V_{ub}|$ and $|V_{cb}|$. The input values used are given in Table 3. We show the graphical results as domains of $\geq$ **5% CL** in Fig. 15.

Parameter	Value ± Error(s)	Source
$\lvert V_{ud}\rvert$	0.97394 ± 0.00089	neutron and nuclear β decay
$\lvert V_{us}\rvert$	0.2200 ± 0.0025	$K \to \pi\ell\nu$ decays
$\lvert V_{ub}\rvert$	$(4.08 \pm 0.61 \pm 0.47) \times 10^{-3}$	LEP inclusive
$\lvert V_{ub}\rvert$	$(4.08 \pm 0.56 \pm 0.40) \times 10^{-3}$	CLEO inclusive & moments $b \to s\gamma$
$\lvert V_{ub}\rvert$	$(3.25 \pm 0.29 \pm 0.55) \times 10^{-3}$	CLEO exclusive
$\lvert V_{cd}\rvert$	0.224 ± 0.014	di-muon production: νN (DIS)
$\lvert V_{cs}\rvert$	0.969 ± 0.058	$W \to X_c X$ (OPAL)
$\lvert V_{cb}\rvert$	$(40.4 \pm 1.3 \pm 0.9) \times 10^{-3}$	excl./incl. & CLEO moments analysis
$\lvert\epsilon_K\rvert$	$(2.271 \pm 0.017) \times 10^{-3}$	PDG 2002
Δm_d	$(0.496 \pm 0.007)\ \mathrm{ps}^{-1}$	*BABAR*, Belle, CDF, LEP, SLD (2002)
Δm_s	Amplitude spectrum 2002	
$\sin 2\beta_{\mathrm{WA}}$	0.734 ± 0.055	*BABAR*, Belle, CDF
m_c	(1.3 ± 0.1) GeV	PDG 2000
$m_t(\overline{\mathrm{MS}})$	(166.0 ± 5.0) GeV	CDF, D0 (PDG 2000)
m_K	(493.677 ± 0.016) MeV	PDG 2002
Δm_K	$(3.4885 \pm 0.0008) \times 10^{-15}$ GeV	PDG 2002
m_{B_d}	(5.2794 ± 0.0005) GeV	PDG 2002
m_{B_s}	(5.3696 ± 0.0024) GeV	PDG 2002
m_W	(80.423 ± 0.039) GeV	PDG 2000
G_F	$(1.16639 \pm 0.00001) \times 10^{-5}\ \mathrm{GeV}^{-2}$	PDG 2002
f_K	(159.8 ± 1.5) MeV	PDG 2002
B_K	$0.86 \pm 0.06 \pm 0.14$	CERN CKM workshop 2002
η_{cc}	1.46 ± 0.41	Herrlich & Nierste; update: CERN CKM workshop
η_{ct}	0.47 ± 0.04	Herrlich & Nierste; update: CERN CKM workshop
η_{tt}	0.573 ± 0.007	Buras, Jamin, Weisz; update: CERN CKM workshop
$\eta_B(\overline{\mathrm{MS}})$	0.55 ± 0.01	Buras *et al.*
$f_{B_d}\sqrt{B_d}$	$(230 \pm 28 \pm 28)$ MeV	Lattice 2000
ξ	$1.16 \pm 0.03 \pm 0.05$	Lattice 2000

Table 3: *Inputs to the global CKM fit. If not stated otherwise: for two errors given, the first is statistical and accountable systematic and the second stands for systematic theoretical uncertainties. In general, measurements with non-vanishing systematic theoretical errors have a floating theoretical component. Theoretical parameters with significant errors are necessarily floating. Upper part: experimental determinations of the CKM matrix elements. Middle upper part: CP-violating and mixing observables. Middle lower part: parameters of the SM predictions obtained from experimental data. Lower part: parameters of the SM predictions obtained from theory.*

References

[1] A. Höcker, H. Lacker, S. Laplace and F. Le Diberder, *Eur. Phys. J.* **C21**, 225, 2001 [hep-ph/0104062] (see also BAD #153); for updated plots and results, visit the CKMfitter site on the web: http://ckmfitter.in2p3.fr

[2] *BABAR* Collaboration (B. Aubert *et al.*), *Phys. Rev. Lett.* **88** (2002) 231801

[3] *BABAR* Collaboration, "*The BABAR Physics Book*", (P. Harrison and H. Quinn eds.) (2002)

[4] F. Bianchi *et al.*, "*Analysis of CP asymmetries in $B \to h^{+}h'^{-}$ decays*", BAD #224

[5] J. Charles, *Phys. Rev.* **D59** 054007, 1999 [hep-ph/9806468]

[6] L. Wolfenstein, *Phys. Rev. Lett.* **51** (1983) 1945

[7] A.J. Buras, M.E. Lautenbacher and G. Ostermaier, *Phys. Rev.* **D50** (1994) 3433

[8] M. Gronau and D. London, *Phys. Rev. Lett.* **65** 3381, 1990

[9] Y. Grossman and H.R. Quinn, *Phys. Rev.* **D58** (1998) 017504

[10] M. Gronau, D. London, N. Sinha, R. Sinha, "*Improving Bounds on Penguin Pollution in $B \to \pi\pi$*", TECHNION-PH-2001-27, UdeM-GPP-TH-01-89, IMSc-2001/05/27, [hep-ph/0105308]

[11] M. Gronau, J. L. Rosner, *Phys. Rev.* **D65** (2002) 013004; Erratum-ibid. D65 (2002) 079901

[12] K. Hagiwara *et al.*, *Phys. Rev.* **D66**, 010001 (2002)

[13] M. Beneke, G. Buchalla, M. Neubert, C. T. Sachrajda *Nucl. Phys.***B606** 245, 2001

[14] Y.-Y. Keum, H.-n. Li, A. I. Sanda *Phys. Lett.***B504** 6, 2001

[15] M. Ciuchini *et al.*, *Phys. Lett.***B515** 33, 2001

[16] *BABAR* Collaboration (B. Aubert *et al.*), hep-ex/0207055, ICHEP'2002

[17] Belle Collaboration (K. Abe *et al.*), hep-ex/0204002 (accepted for publication in PRL)

[18] *BABAR* Collaboration (B. Aubert *et al.*), hep-ex/0207065

[19] *BABAR* Collaboration (B. Aubert *et al.*), hep-ex/0207063

[20] *BABAR* Collaboration (B. Aubert *et al.*), hep-ex/0206053

[21] *BABAR* Collaboration (B. Aubert *et al.*), hep-ex/0109005

[22] Belle Collaboration (B.C.K. Casey *et al.*), hep-ex/0207090

[23] K. Suzuki for the Belle Collaboration, Talk given at the the 31st International Conference on High Energy Physics (ICHEP'02), Amsterdam, The Netherlands (2002)

[24] CLEO Collaboration (D. Cronin-Hennessy *et al.*), hep-ex/0001010

[25] CLEO Collaboration (D.M. Asner *et al.*), Phys.Rev. D65 (2002) 031103

[26] CLEO Collaboration (S. Chen *et al.*), Phys.Rev.Lett.85:525-529,2000

[27] A. Bevan, "*A long term planning study on using the Grossman-Quinn bound*", BAD #504